Subphthalocyanines and Subnaphthalocyanines: Nonlinear Quasi-Planar Octupolar Systems with Permanent Polarity

Guillermo Martín, Gema Rojo, and Fernando Agulló-López*,†

Departamento de Física de Materiales (C-IV), Universidad Autónoma de Madrid, 28049-Madrid, Spain

Víctor R. Ferro and José M. García de la Vega*,‡

Departamento de Química Física Aplicada (C-XIV), Universidad Autónoma de Madrid, 28049-Madrid, Spain

M. Victoria Martínez-Díaz and Tomás Torres*,§

Departamento de Química Orgánica (C-I), Universidad Autónoma de Madrid, 28049-Madrid, Spain

Isabelle Ledoux and Joseph Zyss

Laboratoire de Photonique Quantique et Moléculaire, Ecole Normale Supérieure de Cachan, 94235 Cachan, France

Received: March 15, 2002; In Final Form: October 4, 2002

The second-harmonic generation (SHG) response of unsubstituted subnaphthalocyanines (SubNcs) has been measured for the first time by electric field-induced second-harmonic generation (EFISH) (1.064 and 1.90 μm) and hyper-Rayleigh scattering (HRS) (1.064 μm) experiments. The quadratic hyperpolarizability derived from the experiments is significant ($\beta_{HRS}(0) = 34.7 \times 10^{-30}$ esu) and similar to that also measured under the same conditions for the related unsubstituted subphthalocyanine (SubPc) molecule ($\beta_{HRS}(0) = 38.3 \times 10^{-30}$ esu). To meaningfully discuss the nonlinear optical (NLO) data, semiempirical INDO/S calculations of the permanent dipole moments of the ground and excited states (Q band) have been performed. Moreover, the dipolar transition moments connecting the ground and degenerate excited states and the two excited states have been also determined. The calculations suggest that for those low-energy excited states responsible for the Q optical absorption band, the two molecules (SubPc and SubNc) behave very approximately as planar π-conjugated octupoles with D_{3h} symmetry but having a permanent dipole moment along the perpendicular halogen−boron axis. The charge distribution along this axis is not appreciably influenced by the optical excitation, that is, light-induced charge motion only occurs inside the macrocycle without significant contribution of the apical Cl atom. The β_{HRS} and γ_{EFISH} data have been quantitatively analyzed with a three-level model, taking into account that only electronic terms contribute to the EFISH hyperpolarizability. As a consequence of this analysis, a sound rationale to describe the NLO behavior of these Pc-related compounds (SubPcs and SubNcs) has now emerged.

1. Introduction

Molecular photonics is a rapidly growing field that is reaching maturity. In particular, organic compounds and polymers are starting to be considered as efficient alternatives to inorganic materials for nonlinear optical (NLO) applications, such as electrical and all-optical modulation and switching.[1−4] Phthalocyanines (Pcs) are a class of centrosymmetric highly conjugated molecular systems that have been successfully used for third-order processes including four-wave mixing, third-harmonic generation, and optical limiting.[5−9] For second-order NLO devices, two main strategies[10] have been pursued to introduce the required noncentrosymmetry in Pcs: peripheral substitution of the macrocycle and intrinsic modification of the macrocycle. Another very promising approach[11−15] that combines both strategies is exemplified by subphthalocyanines (SubPcs). They consist of three coupled isoindole units containing boron as central atom and have a delocalized 14 π-electron system. Unlike the related planar Pcs, SubPcs have a pyramid-shaped structure, as determined by X-ray experiments[16,17] and quantum chemical calculations,[18−21] that does not prevent them from having an aromatic nature. High second-harmonic generation (SHG) responses have been obtained in solution through hyper-Rayleigh scattering (HRS) experiments. Moreover, experiments have suggested that the SHG response was mostly octupolar (corresponding to the triangular macrocycle in the "*xy*" plane) so the purely axial (*z*) component of the beta tensor, β_{zzz}, was negligible. Therefore, octupolarity is an additional interesting feature of SubPcs that should be further explored. It is to be mentioned that octupolar molecules may present high SHG responses and offer a new route for optimization.[22−24]

The purpose of this work is to extend the experimental SHG investigation performed on SubPcs[13] to the unsubstituted subnaphthalocyanine (SubNc) with the aim of understanding the effect of increasing the number of benzene rings. So far

* To whom correspondence should be addressed.
† E-mail: fal@uam.es.
‡ E-mail: delavega@uam.es.
§ E-mail: tomas.torres@uam.es.

10.1021/jp020711e CCC: $22.00
Published on Web 12/04/2002

and to the best of our knowledge, no second-harmonic (SHG) data have been reported for the latter molecule. To provide a well-founded and rigorous analysis of the NLO experiments, detailed semiempirical calculations have been performed for both the unsubstituted SubPc and SubNc molecules. The optimization of molecular geometry, as well as the calculation of the electric dipole moments for the ground and lowest excited states, the relevant HOMO and LUMO orbitals, and the optical transition moments, has been carried out. The analysis offers a clear picture of the electronic structure of the two molecules extending some previous quantum chemistry calculations.[18−21,25,26] Moreover, it has provided an interesting rationale for the experimental NLO results obtained on this class of compounds.[13−15] Consequently, a unified picture of the NLO behavior of both families, SubPcs and SubNcs, is now emerging.

2. Experimental Section

Few methods for synthesizing SubNcs have been reported.[14,27,28] They all involve a reaction between 2,3-naphthalenedicarbonitrile and BCl_3 in different solvent mixtures. Using our procedure,[14] we are able to obtain reasonable amounts of pure product (35%) after purification of the crude by column chromatography using toluene as eluent. In addition, we have observed peripheral halogenation of the macrocycle that reduces dramatically the yield of the reaction even when 1-methylnaphthalene was employed as cosolvent.

The UV−visible absorption spectra were measured in toluene solution with a Perkin-Elmer model Lambda 6 spectrophotometer. Electric field-induced second-harmonic generation (EFISH) experiments were performed at two wavelengths, 1064 and 1900 nm. The first wavelength corresponds to the emission of a Q-switched Nd:YAG laser, and the second one was obtained by Raman shifting that emission in a high-pressure hydrogen cell (60 bar). A liquid cell with thick windows in the wedge configuration[29,30] was used to determine a Maker fringes pattern. The incident beam was synchronized with a DC field to induce the breaking of centrosymmetry.

HRS experiments[31−33] were carried out by measuring the intensity of the second-harmonic scattered light when focusing an intense laser beam at 1064 nm on the molecules in chloroform solution. No evidence of spurious contribution of multiphoton-induced fluorescence was obtained.

3. Computational Details

The molecular electronic structures of both unsubstituted SubPc and SubNc were theoretically studied at semiempirical level. First, geometry optimizations were carried out for the considered compounds, and second, single-point calculations were performed over the optimized geometries. The single-point calculations were carried out to determine the electronic structure of the compounds and to account for the electronic UV−visible spectra.

The structures were optimized using the AM1 method[34] implemented in the MOPAC program package (version 6.0).[35] The geometry optimization procedure employed was the "eigenvector following" (EF).[36] The optimization threshold for the value of gradient norm was fixed to 0.01 kcal/mol (Å or radians). The maximum step size allowed during the optimization procedure was 0.02 (Å or radians).

The calculation of the dipole moments of the SubPc and the SubNc in both the ground and the lowest-lying excited states, as well as the dipole moments of the transition among these states, was performed with the INDO method[37] included in the HyperChem (version 5.1)[38] graphic interface, whereas

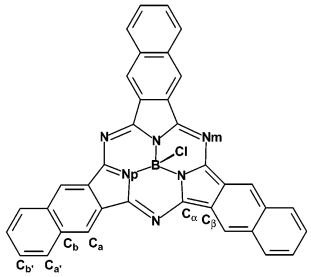

Figure 1. Molecular representation of SubNc. Nm = meso-type nitrogen atom; Np = pyrrolic-type nitrogen atom; C_α and C_β indicate the carbon atoms at the α and β positions of the pyrrol ring; C_a, C_b, $C_{a'}$, and $C_{b'}$ represent the distinct carbon atoms of the naphthalene fused ring.

SCHEME 1: Three-Level Model and Nomenclature Used in the Present Work To Designate the Electronic States.

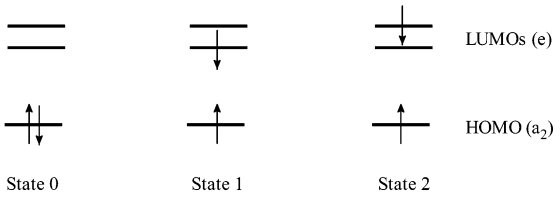

the electronic UV−visible spectra were calculated using the CNDO/S method[39] (implemented by the NDOL, TV-HAVANA package[40]). For these calculations, the configuration interaction was considered using both the six highest occupied and the six lowest unoccupied molecular orbitals that are responsible for the two main bands in the UV−visible spectra of the studied compounds, the Q and B bands.[18,20,25,26]

The electronic properties of the excited states have been calculated over the optimized geometry of the ground state. This decision is based on the fact experimentally proved[13,31] that molecular geometry of the SubPc does not significantly change with the excitation. Kipp et al.[41] have measured small shifts (in the interval between 564 and 578 nm) for the Q-band maxima of the dodecaflorine−SubPc using a number of solvents with different polarities, whereas small Stokes shifts have been measured for the emission of different SubPcs in fluorescence studies.[13] This result was also corroborated by us at semiempirical level performing a preliminary optimization of the molecular geometry for the singly excited state of both molecules using AM1 method. The corresponding geometries only slightly changed with respect to those of the ground states.

We have previously reported[18−21] theoretical calculations of the SubPcs even at higher computational level than that employed in the present work. Nevertheless, we have included here the information about the molecular electronic structure of the SubPc to compare with the results obtained for the SubNc. Figure 1 and Scheme 1 contain the molecular representation of the SubNc and the nomenclature used in this work to designate both the atoms in the molecules and the considered electronic states. States 0, 1, and 2 identify the ground and the lowest-lying excited states, respectively.

4. Molecular Electronic Structure

Figure 2 displays the ground-state optimized structures of SubPcs and SubNcs that are in agreement with previous reports.[16−21] Both the SubPc and the SubNc have the nonplanar pyramid-shaped structural arrangement that characterizes the three isoindole macrocycles. Table 1 shows the values of some selected geometrical parameters. The magnitude δ (which is

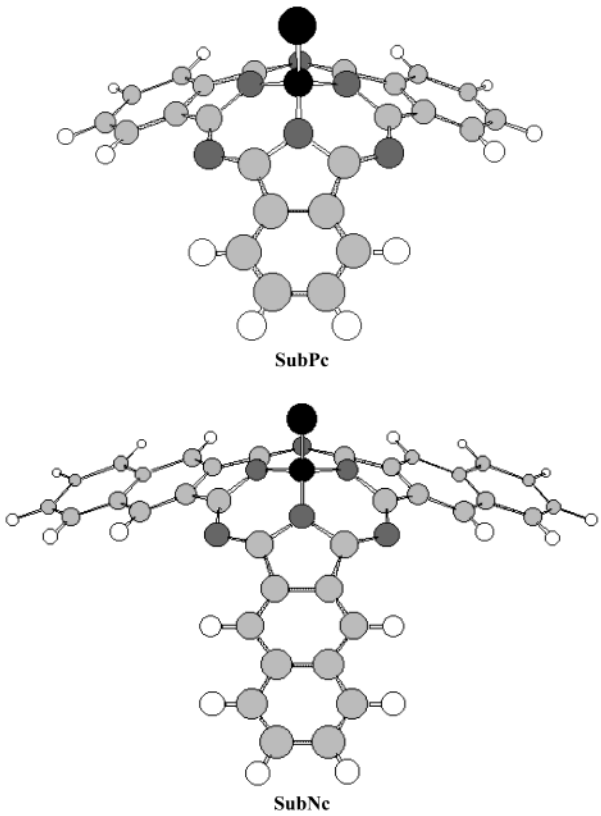

Figure 2. AM1-optimized geometries of the SubPc and the SubNc. Hydrogens are in white, carbons in light gray, nitrogens in dark gray, and both boron and chlorine in black.

defined in Table 1) is included for evaluating the nonplanarity of the molecules. To standardize the results, the plane "*xy*" in this work is determined by the meso nitrogens of the macrocycle. The position of the *x* (connecting two meso nitrogens) and *y* axes is introduced in Figure 1. From Table 1, it is evident that molecular geometries do not significantly differ from one molecule to the other one. The central part of the macrocycle remains unmodified when a second benzene group is added to the isoindole units. The major geometrical changes are observed in the most external part of the macrocycle, that is, in the benzene rings.

The studied molecules may be geometrically considered as pyramids. In correspondence, three parameters are used for quantifying their dimensions: (i) the length of the pyramid base, (ii) the length of the side, and (iii) the opening angle of the pyramid. These parameters are measured, respectively, in this work as the mean values of (i) the distance between the opposite terminal hydrogen atoms of the benzene groups, (ii) the distance between the apical Cl atom and the terminal hydrogen atoms, and (iii) the nonbonding angle $H_{benzene}-Cl-H_{benzene}$. Table 2 compares the dimensions of both pyramids. The length of the pyramids is proportional to the number of benzene groups constituting the molecules, whereas the opening angle is less sensible to the compositional changes observed in these molecules. This result points forward to the rigidity of the three isoindole macrocycle.

Table 3 gives the ground state (0) dipole moments for both molecules calculated by the INDO method. They are similar in magnitude and oriented along the B−Cl (*z*) axis as expected from symmetry (no significant contributions along the *x* and *y* axes have been obtained). The dipole moments for the lowest degenerated excited states (1 and 2) of both molecules are also included in Table 3. The values of the dipole moments of the excited states are close to those determined for the ground states (Table 3), suggesting that no significant electronic reordering takes place during the excitations. This result is in agreement with the experimental[13,31,41] evidences referred to in the previous section. From here, it is inferred that charge motion is mostly restricted to the macrocycle, the apical Cl only playing a passive role.

TABLE 1: Calculated Values for Some Selected Geometrical Parameters of the SubPc and SubNc

Bond Distances (Å)		
geometrical parameters	SubPc	SubNc
B−Cl	1.822	1.822
B−Np	1.540	1.540
Np−C_α	1.408	1.406
Nm−C_α	1.359	1.359
$C_\alpha-C_\beta$	1.477	1.479
$C_\beta-C_\beta$	1.444	1.462
$C_\beta-C_a$	1.386	1.366
C_a-C_b	1.398	1.425
C_b-C_b	1.398	1.423
$C_b-C_{a'}$		1.423
$C_{a'}-C_{b'}$		1.373
$C_{b'}-C_{b'}$		1.416
Bond Angles (deg)		
geometrical parameters	SubPc	SubNc
N−B−Cl	110.7	110.8
Np−B−Np	108.2	108.2
B−Np−C_α	121.1	121.1
Np−$C_\alpha-C_\beta$	105.2	105.3
Np−C_α−Nm	124.8	124.8
$C_\alpha-C_\beta-C_\beta$	107.3	107.0
C_α−Nm−C_α	116.7	116.7
$C_\beta-C_\beta-C_a$	120.5	120.9
$C_\beta-C_a-C_b$	118.2	118.8
$C_a-C_b-C_b$	121.3	120.4
$C_b-C_{a'}-C_{b'}$		120.7
Mean Atomic Deviations with Respect to the Plane NmNmNm (Å)		
	SubPc	SubNc
δ^b	0.77	1.21

[a] The mean values of the corresponding individual parameters are considered. [b] $\delta = \sum|r_z|/n$, where r_z is the *z* coordinate of each atom of the molecule when the *xy* plane is defined by the three meso nitrogens. The summation runs over the 28 atoms of the SubPc and the 40 atoms of the SubNc skeletons. The H atoms in peripheral position, as well as the axial halogen ligand, were excluded.

TABLE 2: Dimensions of the Pyramidal Arrangement Corresponding to the SubPc and SubNc

	SubPc	SubNc
pyramid side, Å	8.1	10.5
pyramid base, Å	11.0	14.8
opening angle, deg	85.5	90.0

TABLE 3: INDO Calculations for the Permanent Dipole Moments of the Ground and Lowest-Lying Excited States of the SubPc and SubNc

		permanent dipole moments (D)			
molecule	state	μ_x	μ_y	μ_z	μ_{TOTAL}
SubPc	0	0.00	−0.01	−6.73	6.73
SubNc	0	0.00	−0.01	−6.77	6.77
SubPc	1	−0.90	−0.01	−6.81	6.87
SubNc	1	0.41	0.99	−6.96	7.04
SubPc	2	0.88	0.01	−6.81	6.87
SubNc	2	−0.41	−0.98	−6.81	6.89

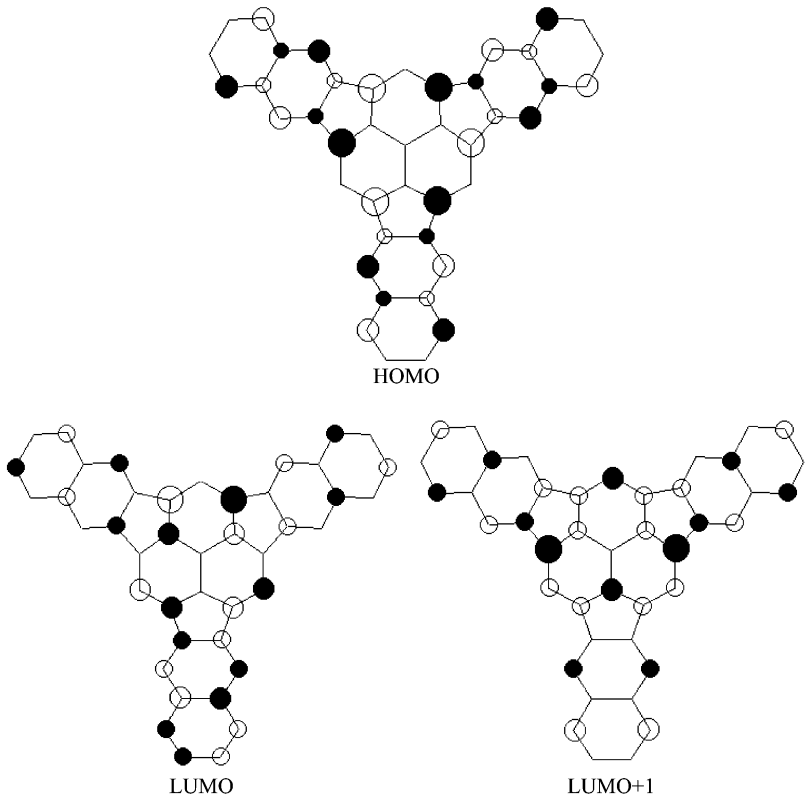

Figure 3. Atomic contributions both to the highest occupied molecular orbital (HOMO) and to the two low-lying unoccupied molecular orbitals (LUMOs) in the SubNc. For notation, see the text.

It is interesting to identify the contributions to the ground- and excited-state moments arising from the B−Cl axis and from the pyramidal macrocycle structure. This problem is partially analyzed in ref 21. Nevertheless, in the present work, the values in Table 3 were compared with those determined for the same molecules ignoring the apical Cl. One sees that the B−Cl bond makes the most significant contribution to the dipole moments. Moreover, the molecular fragments conformed by the B−Cl bond and the three B−Np bonds practically reproduce the total dipole moments of the molecules.

Figure 3 shows the profiles for the HOMO, LUMO, and LUMO + 1 molecular orbitals in SubNc. They represent the atomic orbitals contributions to the molecular orbitals. The color of the circle indicates the sign of the *Ci*. White ones correspond to $Ci > 0$. The diameter of the circles is proportional to the absolute value of the *Ci*, which is defined as $Ci = \sum c_i$, where c_i are the coefficients for each atom in the expression where the molecular orbital (Φ_i) is defined as a linear combination of atomic orbitals (ϕ_i): $\Phi_i = \sum c_i \phi_i$. It is important to notice that "p_z" atomic orbitals predominantly contribute to the considered molecular orbitals indicating that, despite the nonplanar pyramidal shape, these orbitals are mostly π-type accounting for the molecular aromaticity. There is no contribution to these orbitals coming from the apical Cl. The frontier orbitals for SubNc are very similar to those reported for SubPc.[18−21] For the symmetry group of this molecule (C_{3v}), the HOMO corresponds to the irreducible representation a_2, whereas the LUMO and LUMO + 1, which are energetically degenerated, belong to the e symmetry representation.

The corresponding orbital energies are given in Table 4. From these data, it can be inferred that the HOMO of the SubNc is less stable than the one of SubPc, probably due to the increasing conjugation of the system. The *gap* between the HOMO and LUMO, defined as the difference of the corresponding molecular orbital energies, decreases from the SubPc (6.98 eV) to the SubNc (6.38 eV).

TABLE 4: Calculated (CNDO/S) Orbital Energies

	energies (eV)	
orbitals (symmetry)	SubPc	SubNc
LUMO + 1 (e)	−2.79	−2.77
LUMO (e)	−2.79	−2.76
HOMO (a_2)	−6.62	−6.29
HOMO − 1 (a_1)	−9.59	−9.00

5. Optical Absorption Spectra

Optical absorption spectrum of the unsubstituted SubNc in toluene solution is similar to that of SubPc, Figure 4, (and also to those of Pcs and porphyrins) and presents two main bands: the lowest energy band in the red region of the spectrum and the more energetic one in the near UV. These bands are designated, respectively, Q and B by analogy with porphyrins despite the structural and electronic differences between these molecular systems (see refs 18, 25, and 26). As discussed in ref 26, the peak of the Q band of the SubNc is shifted to lower energies and the strength is enhanced in comparison to SubPcs because of the extended conjugation. The observed red shift agrees with the fact revealed by the theoretical calculations that the gap of the SubNc is 0.5 eV smaller than the gap of the SubPc.

Our calculations have confirmed that the Q band corresponds to an a_2(HOMO) → e(LUMO) transition. It appears that the band is essentially π-type despite the molecular buckling, suggesting that the apical Cl atom does not play a significant role in the transition. Moreover, the transition dipole moment lies in the macrocycle mean plane (x,y) perpendicular to the B−Cl axis.

The energies of the optical Q and B transitions have been determined and are given in Table 5, together with the

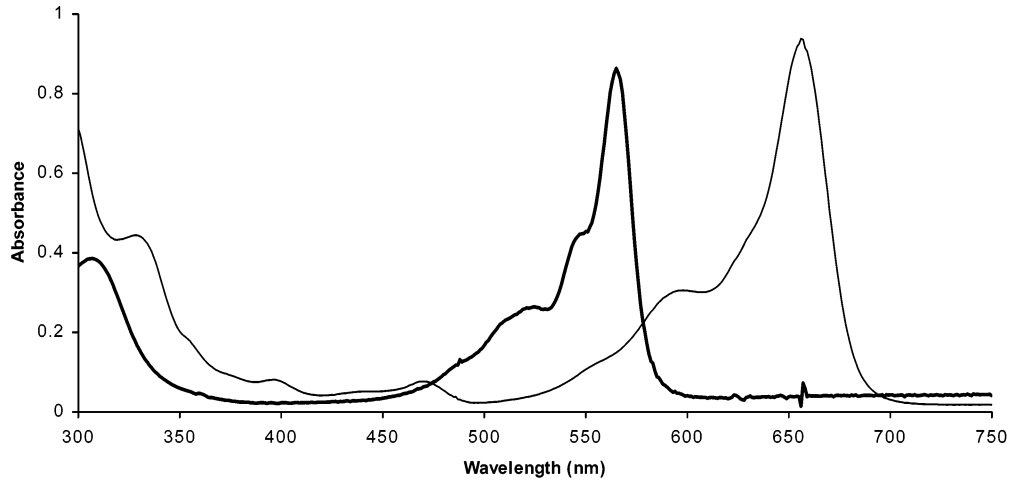

Figure 4. UV−vis spectra of SubNc (thin line) and SubPc (solid line) in toluene.

TABLE 5: Experimental and Calculated (CNDO/S) Peak Wavelengths and the Extinction Coefficients for the Q and B Transitions

	experimental		calculated	
transition	λ_{max} (nm)	log ϵ	λ_{max} (nm)	log ϵ
		SubPc		
Q	584	4.95	682	4.52
B	305	4.70	279	4.87
		SubNc		
Q	660	4.97	766	4.57
B	299	4.90	307	3.05

TABLE 6: INDO Results for the Dipole Moments Transitions of All Three-Level Transitions in Both SubPc and SubNc

		transition dipole moments (D)			
molecule	transition	μ_x	μ_y	μ_z	μ_{TOTAL}
SubPc	0 → 1	5.63	5.62	0.00	7.95
SubNc	0 → 1	−9.73	−1.96	0.01	9.93
SubPc	0 → 2	5.62	−5.63	0.00	7.95
SubNc	0 → 2	−1.97	9.79	−0.01	9.98
SubPc	1 → 2	5.55	−6.11	−0.16	8.25
SubNc	1 → 2	7.58	8.44	−0.11	11.30

experimental values. The calculated transition energies are not in good accordance with those measured values although they reproduce the principal trends experimentally observed. It may be explained by the fact that the orbitals involved in these transitions are not pure π molecular orbitals but also include contributions of the s, p_x, and p_y atomic orbitals because of the molecular nonplanarity. The theoretical methods used in the calculation of the electronic transition energies attribute an important contribution of the σ-bonding components to the transition energy.

The dipole moments for the transitions 0 → 1, 0 → 2, and 1 → 2 using the INDO methods are given in Table 6. This latter moment is essential for a three-level description of the NLO response presented in the following section. All transition moments are similar in magnitude indicating that they occur among the same parts of the molecules (the macrocycle) as suggested by the profiles of the molecular orbitals involved in these transitions (see Figure 3). The dipole moments for the transitions in SubNc are always larger than those obtained for SubPc in correspondence with the major extension of the π system.

One main conclusion of the theoretical calculations is that for the lowest electronic excitations (Q and B bands) the dipole transition moments have *x* and *y* components without any significant contribution along the permanent electric dipole (*z* axis) for both SubPcs and SubNcs. They essentially behave as octupolar conjugated molecules with charge motion inside the macrocycle plane. However, they present a permanent dipole moment along the *z* (B−Cl) axis that could be advantageously used to achieve molecular orientation and poling. One should also note that the following relations among the transition dipole components are very approximately obeyed in accordance with symmetry arguments for the D_{3h} group:[24]

$$|\mu_x(0\rightarrow 1)| = |\mu_y(0\rightarrow 2)|$$

$$|\mu_y(0\rightarrow 1)| = |\mu_x(0\rightarrow 2)|$$

TABLE 7: Calculated and Experimental Quadratic Hyperpolarizability, β_{HRS}, Values in Units of 10^{-30} esu

	calculated		experimental	
compound	β_{xxx}(1.06)	β_{HRS}(1.06)	β_{HRS}(0)	β_{HRS}(1.06)
SubPc	164	101	38.3	92
SubNc	109	67.1	34.7	41

TABLE 8: Calculated and Experimental γ_{EFISH} Values in Units of 10^{-33} esu

compound	γ_{calcd}(1.06)	γ_{exptl}(1.06)	γ_{calcd}(1.9)	γ_{exptl}(1.9)
SubPc	1.1	−9.75	1.19	−2.86
SubNc	0.46	9.52	10.5	−5.96

6. SHG Susceptibilities

The calculated and experimental β_{HRS} data at 1064 nm and the γ_{EFISH} susceptibilities at 1064 and 1900 nm for unsubstituted SubPc and SubNc are presented in Tables 7 and 8, respectively. For a purely octupolar molecule, the orientational contribution to γ_{EFISH} should vanish, so the measured value should correspond to the electronic contribution. Therefore, the information on the beta tensor is almost exclusively included in the β_{HRS}. For the unsubstituted SubPc, the β_{HRS} at $\lambda = 1.06$ μm are in the range (although somewhat larger) previously found[13] for donor-doped SubPc at $\lambda = 1.46$ μm. On the other hand, the value measured for the unsubstituted SubNc is about a factor 2 smaller. However, as we will see below, the two values become approximately equal when the SHG response is extrapolated at $\omega = 0$.

The essentially octupolar nature of our molecules demands (at least) a three-level model.[24,41] In principle, because of the predominance of the Q band in the absorption spectrum, it

appears reasonable to consider the ground (0) and the two lowest degenerate excited states (1, 2). If we assume, in accordance with the considerations given above, that molecular symmetry is D_{3h}, the nonzero components of the β tensor are $\beta_{xxx} = -\beta_{xyy} = -\beta_{yyx} = -\beta_{yxy}$ with[24,42]

$$\beta_{xxx} = \frac{3\omega_{01}{}^2[\Delta\mu^x_{01}((\mu^x_{01})^2 - (\mu^y_{02})^2) - 2\mu^x_{01}\mu^x_{02}\mu^x_{12}]}{2\hbar^2(\omega_{01}{}^2 - \omega^2)(\omega_{01}{}^2 - 4\omega^2)} \quad (1)$$

where damping corrections have been ignored. In expression 1, $\Delta\mu^x_{01}$ represents the x component of the change in dipole moment between states 0 and 1 (see Table 3). On the other hand, for a planar molecule with symmetry D_{3h}, the quadratic HRS hyperpolarizability is given by:[42]

$$\langle\beta_{\mathrm{HRS}}\rangle = 2\sqrt{\frac{2}{21}}\beta_{xxx} \quad (2)$$

where the x axis is perpendicular to one of the mirror planes. Introducing into expressions 1 and 2 the parameters obtained from the semiempirical calculations, one arrives at the final values for the β_{xxx} and β_{HRS} listed in Table 7. It also includes the experimental results to facilitate comparison.

From that analysis, it is concluded that our calculations using the INDO parameters correctly describe the experimental trend and account for the superior β_{HRS} value found for the SubPc over that for the SubNc at $\lambda = 1.06\ \mu$m. On the other hand, the quantitative agreement between theory and experiment is acceptable, although the theoretical values are larger by 10% (for SubPc) and 60% (for SubNc). The differences may be considered reasonable taking into account the neglect of damping factors and higher electronic levels in eq 1, as well as the approximations involved in the quantum-chemistry semiempirical methods. The role of damping factors can be easily taken into account by substituting the complex frequencies $\omega_{01} = \omega_{02} = \omega_{01} + i\Gamma$ for the real ones $\omega_{01} = \omega_{02}$ appearing in eq 1 and using the bandwidth Γ that can be derived from the experimental spectra. No appreciable improvement in β_{HRS} has been achieved. Finally, our theoretical framework allows us to determine the β_{HRS} values at $\omega = 0$ that are also included in Table 7. It comes out that at low frequencies (i.e., off-resonance) SubPc and SubNc show an essentially similar SHG performance. The differences found at $\lambda = 1.06\ \mu$m are mostly caused by frequency dispersion.

The analysis of the γ_{EFISH} data is more complicated. Although it is not the main objective of this work, we have calculated the values of the electronic contributions to γ_{EFISH} using the corresponding formula for D_{3h} symmetry. The expression for the electronic contribution to γ_{EFISH} is

$$\gamma_{\mathrm{elec}} = \frac{8}{30\hbar^3}[|\vec{\mu}_{01}|^2|\vec{\mu}_{12}|^2]\sum_{i=1}^{6} D^i_{111} - \frac{7}{30\hbar^3}[|\vec{\mu}_{01}|^4]\sum_{i=1}^{3} d^i_{11} \quad (3)$$

where the D^i_{111} and d^i_{11} are the appropriate resonance factors given next:

$$\sum_{i=1}^{6} D^i_{111} = \frac{6\omega_{01}{}^3(2\omega_{01}{}^2 - 5\omega^2)}{(\omega_{01}{}^2 - 4\omega^2)^2(\omega_{01}{}^2 - 4\omega^2)^2}$$

$$\sum_{i=1}^{3} d^i_{11} = \frac{12\omega_{01}}{(\omega_{01}{}^2 - 4\omega^2)(\omega_{01}{}^2 - 4\omega^2)} \quad (4)$$

Results are given in Table 8. The agreement with the experiment is very poor. In particular, the theoretical nearly off-resonant values (at $\lambda = 1.90\ \mu$m) are very small and positive at variance with the negative sign found in experiment. So, it appears that for γ_{EFISH} the main assumptions used for our semiempirical calculations are much more critical than for β. In other words, calculated values are much more sensitive to errors in the geometrical and electronic parameters of the model. On the other hand, one should take into account that molecules are nonplanar and have pyramidal shape (C_{3v} symmetry) with a dipole moment along the 3-fold z axis (see Table 3). This fact introduces additional nonzero components of the β tensor involving the z axis. Consequently, a dipolar (vector) component for β should contribute to the orientational term in γ_{EFISH}. This orientational term has not been considered in our calculations. Therefore, it is not surprising that the experimental and theoretical values for γ_{EFISH} show a large discrepancy.

7. Concluding Remarks

The main result of the work is that the quadratic hyperpolarizability values (β_{HRS}) for both SubPcs and SubNcs can be understood with a model exclusively including the low-energy Q-band transitions ($0 \rightarrow 1$, $0 \rightarrow 2$, $1 \rightarrow 2$). Moreover, these relevant transitions and so the NLO response can be approximately described by means of a quasi-planar octupolar molecule with D_{3h} symmetry. In particular, the $0 \rightarrow 1$, $0 \rightarrow 2$, and $1 \rightarrow 2$ transition moments mostly have x and y components (within the macrocycle plane) without significant contribution along the z axis. With this model, a reasonable quantitative agreement between theoretical and experimental β_{HRS} values has been achieved for SubPc and SubNc. In fact, the theoretical analysis confirms that the two molecules present similar quadratic NLO responses despite the extended conjugation area for SubNcs. It is also to be remarked that both SubPc and SubNc, in addition to an approximate octupolar character, present moderate permanent dipole moments that permit the application of the electrical poling technique to achieve molecular ordering.[15] Therefore, SubPcs and SubNc constitute interesting compounds for the development of ordered nonlinear optical materials suitable for optoelectronic applications.

Acknowledgment. This work was supported by Grant BQU2001-0152 from the Ministry of Science and Technology, Spain. This work was supported by CICYT (Spain) and the European Community through Research Project MAT-99-0180 and Contract HPRN-CT-2000-00020, respectively.

References and Notes

(1) Zyss, J., Ed. *Molecular Nonlinear Optics: Materials, Physics and Devices*; Academic Press: New York, 1994.

(2) Birge, R. R., Ed. *Molecular and Biomolecular Electronics*; Advances in Chemistry Series 240; American Chemical Society: Washington, DC, 1994.

(3) Lindsay, G. A., Singer, K. D., Eds. *Polymers for Second-Order Nonlinear Optics*; American Chemical Society: Washington, DC, 1995.

(4) Bosshard, Ch.; Sutter, K.; Prêtre, Ph.; Hulliger, J.; Flörsheimer, M.; Kaatz, P.; Günter, P. *Organic Nonlinear Optical Materials*; Advances in Nonlinear Optics, Vol. 1; Gordon and Breach Publishers: Basel, Switzerland, 1995.

(5) Leznoff, C. C., Lever, A. B. P., Eds. *Phthalocyanines: Properties and Applications*; VCH Publishers: Weinheim, Germany, 1989, 1993, 1996; Vols. 1−4.

(6) Nalwa, H. S. *Adv. Mater*. **1993**, *53*, 341.

(7) Nalwa, H. S.; Shirk, J. C. In *Phthalocyanines: Properties and Applications*; Leznoff, C. C.; Lever, A. B. P., Eds.; VCH Publishers: Weinheim, Germany, 1996; Vol. 4, p 79.

(8) Diaz-García, M. A.; Dogariu, A.; Hagan, D. J.; VanStryland, E. H. *Chem. Phys. Lett*. **1997**, *266*, 86.

(9) de la Torre, G.; Vazquez, P.; Agulló-López, F.; Torres, T. *J. Mater. Chem.* **1998**, *8*, 1671.
(10) de la Torre, G.; Torres, T.; Agulló-López, F. *Adv. Mater.* **1997**, *9*, 265.
(11) Meyer, M.; Plenzig, F.; Rauschnabel, J.; Hanack, M.; del Rey, B.; Sastre, A.; Torres, T. *Synthesis* **1996**, 1139.
(12) del Rey, B.; Torres, T. *Tetrahedron Lett.* **1997**, *38*, 5351.
(13) del Rey, B.; Keller, U.; Torres, T.; Rojo, G.; Agulló-López, F.; Nonell, F.; Martí, C.; Brasselet, S.; Ledoux, I.; Zyss, J. *J. Am. Chem. Soc.* **1998**, *120*, 12808.
(14) Nonell, S.; Rubio, N.; del Rey, B.; Torres, T. *J. Chem. Soc., Perkin Trans. 2* **2000**, 1091.
(15) Rojo, G.; del Rey, B.; Torres, T.; Agulló-López, F. *J. Appl. Phys.* **1998**, *84*, 6507.
(16) Kietaibl, H. *Monatsh. Chem.* **1974**, *105*, 405.
(17) Potz, R.; Göldner, M.; Hückstädt, H.; Cornelissen, U.; Tutass, A.; Homborg, H. *Z. Anorg. Allg. Chem.* **2000**, *626*, 588.
(18) Ferro, V. R.; Poveda, L. A.; González-Jonte, R. H.; García de la Vega, J. M.; Torres, T.; del Rey, B. *J. Porphyrins Phthalocyanines* **2000**, *4*, 610.
(19) Ferro, V. R.; García de la Vega, J. M.; González-Jonte, R. H.; Poveda, L. A. *J. Mol. Struct. (THEOCHEM)* **2001**, *537*, 223.
(20) Ferro, V. R.; García de la Vega, J. M.; Claessens, C. G.; Poveda, L. A.; González-Jonte, R. H. *J. Porphyrins Phthalocyanines* **2001**, *5*, 491.
(21) Ferro, V. R.; Poveda, L. A.; Claessens, C. G.; González-Jonte, R. H.; García de la Vega, J. M. *Int. J. Quantum Chem.*, in press.
(22) Joffre, M.; Yaron, D.; Sibley, R. J.; Zyss, J. *J. Chem. Phys.* **1992**, *97*, 5607.
(23) Ledoux, I.; Zyss, J. *Chem. Rev.* **1994**, *94*, 77.
(24) Zyss, J.; Brasselet, S. *J. Nonlinear Opt. Phys. Mater.* **1998**, *7*, 397.
(25) Kobayashi, N. *J. Porphyrins Phthalocyanines* **1999**, *3*, 453.
(26) Kobayashi, N.; Ishizaki, T.; Ishii, K.; Konami, H. *J. Am. Chem. Soc.* **1999**, *121*, 9096.
(27) Stork, J. R.; Potucek, R. J.; Durfee W. S.; Noll, B. C. *Tetrahedron Lett.* **1999**, *40*, 8055.
(28) Zyskowski, C. D.; Kennedy, V. O. *J. Porphyrins Phthalocyanines* **2000**, *4*, 707.
(29) Oudar, J. L. *J. Chem. Phys.* **1977**, *67*, 446.
(30) Kajzar, F.; Messier, J. *Rev. Sci. Instrum.* **1987**, *58*, 2081.
(31) Terhume, R. W.; Maker, P. D.; Savage, C. M. *Phys. Rev. Lett.* **1965**, *14*, 681.
(32) Clays, K.; Persoons, A. *Phys. Rev. Lett.* **1991**, *66*, 2980.
(33) Zyss, J.; Chauvam, T.; Dhenaut, C.; Ledeux, I. *Chem. Phys.* **1995**, *177*, 281.
(34) Dewar, M. J. S.; Zoebisch, E. G.; Healey, E. F.; Stewart, J. P. *J. Am. Chem. Soc.* **1985**, *107*, 3902.
(35) (a) Stewart, J. P. P. *Quantum Chem. Program Exch.* **1990**, 581. (b) Stewart, J. P. P. *J. Comput.-Aided Mol. Des.* **1990**, 4.
(36) Schegel, H. B. Optimization of equilibrium geometries and transition structures. In *Ab Initio Methods in Quantum Chemistry*; Lawley, K. P., Ed. John Wiley & Sons Ltd: Chichester, U.K., 1987; p 250.
(37) Anderson, W. P.; Edwards, W. D.; Zerner, M. C. *Inorg. Chem.* **1986**, *25*, 2728−2731.
(38) *HyperChem.*, release 5.1; Hypercube, Inc.: Gainesville, FL, 1999.
(39) del Bene, J.; Jaffe, G. A. *J. Chem. Phys.* **1968**, *48*, 1807.
(40) Montero, L. A.; Alfonso, L.; Alvarez, J. R.; Perez, E. *Int. J. Quantum Chem.* **1990**, *37*, 465. Program Package available on request.
(41) Kipp, R. A.; Simon, J. A.; Beggs, M.; Ensly, H. E.; Schmehl, R. H. *J. Phys. Chem. A* **1998**, *102*, 5659.
(42) Brasselet, S.; Zyss, J. *J. Nonlinear Opt. Phys. Mater.* **1996**, *5*, 671.